REPORT DOCUMENTATION PAGE

Form Approved
OMB No. 0704-0188

Public reporting burden for this collection of information is estimated to average 1 hour per response, including the time for reviewing instructions, searching existing data sources, gathering and maintaining the data needed, and completing and reviewing this collection of information. Send comments regarding this burden estimate or any other aspect of this collection of information, including suggestions for reducing this burden to Department of Defense, Washington Headquarters Services, Directorate for Information Operations and Reports (0704-0188), 1215 Jefferson Davis Highway, Suite 1204, Arlington, VA 22202-4302. Respondents should be aware that notwithstanding any other provision of law, no person shall be subject to any penalty for failing to comply with a collection of information if it does not display a currently valid OMB control number. **PLEASE DO NOT RETURN YOUR FORM TO THE ABOVE ADDRESS.**

1. REPORT DATE *(DD-MM-YYYY)*	2. REPORT TYPE	3. DATES COVERED *(From - To)*
16-10-2015	Final Report	7/15/2009-7/14/2015

4. TITLE AND SUBTITLE
Heat Measurements in Electrolytic Metal-Deuteride Experiments

5a. CONTRACT NUMBER

5b. GRANT NUMBER
N00173-09-1-G027

5c. PROGRAM ELEMENT NUMBER

6. AUTHOR(S)
Francis Tanzella

Esperanza Alvarez

Michael McKubre

5d. PROJECT NUMBER
P19120

5e. TASK NUMBER

5f. WORK UNIT NUMBER

7. PERFORMING ORGANIZATION NAME(S) AND ADDRESS(ES)

SRI International
333 Ravenswood Ave.
Menlo Park, CA 94025

8. PERFORMING ORGANIZATION REPORT NUMBER

9. SPONSORING / MONITORING AGENCY NAME(S) AND ADDRESS(ES)

10. SPONSOR/MONITOR'S ACRONYM(S)

11. SPONSOR/MONITOR'S REPORT NUMBER(S)

12. DISTRIBUTION / AVAILABILITY STATEMENT
Approved for Public Release, distribution is unlimited.

13. SUPPLEMENTARY NOTES

14. ABSTRACT

Attempts to measure excess energy from both electrolytic and gas phase experiments were made. The electrolytic cells were those designed and built by Dr. V. Violante at ENEA using SuperWave™ stimulation and analyzed using his thermal modeling. Although very high loadings were seen, the excess energy measured was less than the measurement uncertainty. Using Pd in various catalysts (silica, yttria stabilized zirconia, and zeolites) prepared by Dr. D. Kidwell at NRL, we attempted to measure excess energy and He production. After operating tens of experiments, we have found that D_2 exposure to Pd-filled zeolites and $PdNiZrO_x$ catalysts leads to higher temperatures than does H_2 exposure. However, we have not ruled out that this may be due to heat capacity and thermal conductivity differences between the two gases.

15. SUBJECT TERMS
Low Energy Nuclear Reactions, SuperWave™, electrolysis, deuterium, zeolite, silica, yttria stabilized zirconia, palladium.

16. SECURITY CLASSIFICATION OF: UNCLASSIFIED			17. LIMITATION OF ABSTRACT	18. NUMBER OF PAGES	19a. NAME OF RESPONSIBLE PERSON
a. REPORT	b. ABSTRACT	c. THIS PAGE		21	Rachel Stahl
					19b. TELEPHONE NUMBER *(include area code)* 650-859-2004

Standard Form 298 (Rev. 8-98)
Prescribed by ANSI Std. Z39.18

Final Report • October 16, 2015

HEAT MEASUREMENTS IN ELECTROLYTIC METAL-DEUTERIDE EXPERIMENTS

SRI Project No. P19120

Grant No. N00173-09-1-G027

Period of Performance 07/15/2009 – 07/14/2015

Prepared by:

Drs. Francis Tanzella, Esperanza Alvarez, and Michael McKubre
Chemistry and Materials Laboratory
SRI International
333 Ravenswood Avenue
Menlo Park, CA 94025-3493

Prepared for:

U.S. Naval Research Laboratory
Code 6370
4555 Overlook Ave. SW
Washington, DC 20375-5320
Attention: Dr. Kenneth Grabowski

Approved by:

Dr. Martha Berding
Executive Director
Energy & Environment Center
SRI International

ADMINISTRATIVE

SRI International (SRI) spent all of its existing project funds by September 17, 2010. As such, all efforts on this project were suspended at that time until further funds became available. As no new funds became available, this final report covers all efforts on this project through 2010.

PRESENTATIONS

Drs. McKubre and Tanzella attended the 15th International Conference on Condensed Matter Nuclear Science (CMNS) in Rome, Italy from October 4-9, 2009. Dr. McKubre presented results related to the earlier phases of this study. Dr. Tanzella presented results of other CMNS work being performed at SRI. Drs. McKubre and Tanzella took part in many valuable technical discussions related to this project during this conference.

Drs. McKubre and Tanzella each presented papers at the New Energy Technology symposium at the American Chemical Society meeting in San Francisco (March 21 – 25, 2010). After the symposium, Drs. Takahashi, Kitamura, and Hiroki visited SRI for discussions of their latest results from exposing PdZrNi oxides to deuterium gas. Discussions were also held with Drs. Violante, Sarto, Lecci, and Castagna about their latest results from ENEA (the Italian National Agency for New Technologies, Energy and Sustainable Economic Development). Dr. Tanzella visited the Naval Research Laboratory (NRL) for discussions with Drs. Kidwell and Knies on May 14, 2010 after presenting a brief on low-energy nuclear reactions (LENR) at the Energetics Materials Intelligence Seminar in McLean, VA. Dr. McKubre visited NRL for discussions with Drs. Kidwell and Knies on May 25, 2010 during a trip that included a visit to the University of Missouri. Dr. McKubre presented a brief on LENR at the Adelphi Army Research Laboratory in Maryland in late June 2010.

ELECTROLYSIS CELLS WITH "SUPERWAVE®" STIMULATION

A purchase order for cell/calorimeters with high thermal sensitivity and a short time constant for the electrolysis of Pd foils has been executed with ENEA, Frascati. Working closely with ENEA, we have determined that our LL calorimeter is compatible with the ENEA cell/calorimeter and can be used as a sealed, insulated shroud allowing immersion of the ENEA cell/calorimeter in a controlled temperature water bath, if necessary, during mass flow operation. This system will allow us to operate the cells in a manner identical to that performed by the ENEA for calorimetric measurements.

We worked very closely with ENEA, Frascati to ensure that all cell/calorimeter parts that they would deliver were compatible with our LL calorimeter system. All parts should fit and operate well in our immersion, mass-flow calorimeter system.

Cathodes from NRL arrived to be utilized in these new calorimeters.

One cell/calorimeter assembly from ENEA was delivered and assembled in late March along with one Pd foil cathode. The cell/calorimeter assembly that was delivered from ENEA and assembled in late March was integrated into the SRI calorimeter system. Minor modifications were made to accommodate SRI's calorimeter system. Three Pd foils from NRL were also

available for test. After calibration and "shake-down" we planned to work with ENEA to determine which Pd foils available to SRI would be used for further testing. The remaining three cell/calorimeter assemblies from ENEA were delivered in early June. These are identical to the one delivered and assembled in March, so integration with the existing system was not expected to be a problem.

SETUP AND OPERATION

One of the cells from ENEA was set up and operated to obtain calibrations using direct current (DC). The cell's dimensions and configuration are showed in Figure 1. The electrochemical cell exterior (Figure 1a) is comprised of a 25.4-mm dia., 220-mm tall cylindrical stainless steel vessel. The vessel is sealed with a 2.75" ConFlat® fitting with two 0.25" Cajon VCR® fittings that communicate with the headspace. Two platinum anodes (Figure 1b) 40-mm x 25.4-mm x 100-μm form a sandwich with the palladium cathode of similar dimensions with a 6.5-mm anode-cathode distance. This three-electrode structure is positioned at the center of the cell and held by polytetrafluoroethylene (PTFE) structures. At the top, there is a 24.5-mm tall Pd basket for the Pt on Al_2O_3 recombining catalysts.

A leak-free flanged fitting on top completes the cell boundary and acts to reduce vertical conductive heat transfer.

The wiring inside the cell consists of: (1) two current wires to the anode and cathode (the cell voltage is measured just external to the cell), (2) four small wires used to make four terminal measurements of the cathode axial resistance, (3) a 4-wire Pt-100 resistive temperature detector (RTD) to measure the temperature of the electrolyte, (4) the reference electrode, and (5) a ground connection. The electrolytic cell has an Omega pressure transducer and a pressure relief burst disk connected to the Cajon VCR® fittings. A schematic drawing of the electrolytic cell and the calorimetric system is shown in Figure 2.

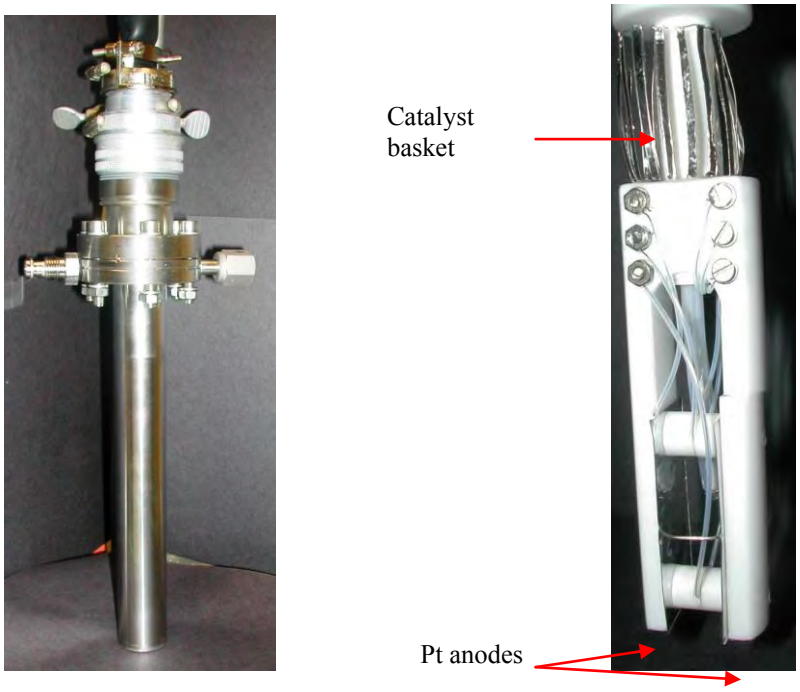

Figure 1. Electrochemical cell: (a) exterior; (b) interior.

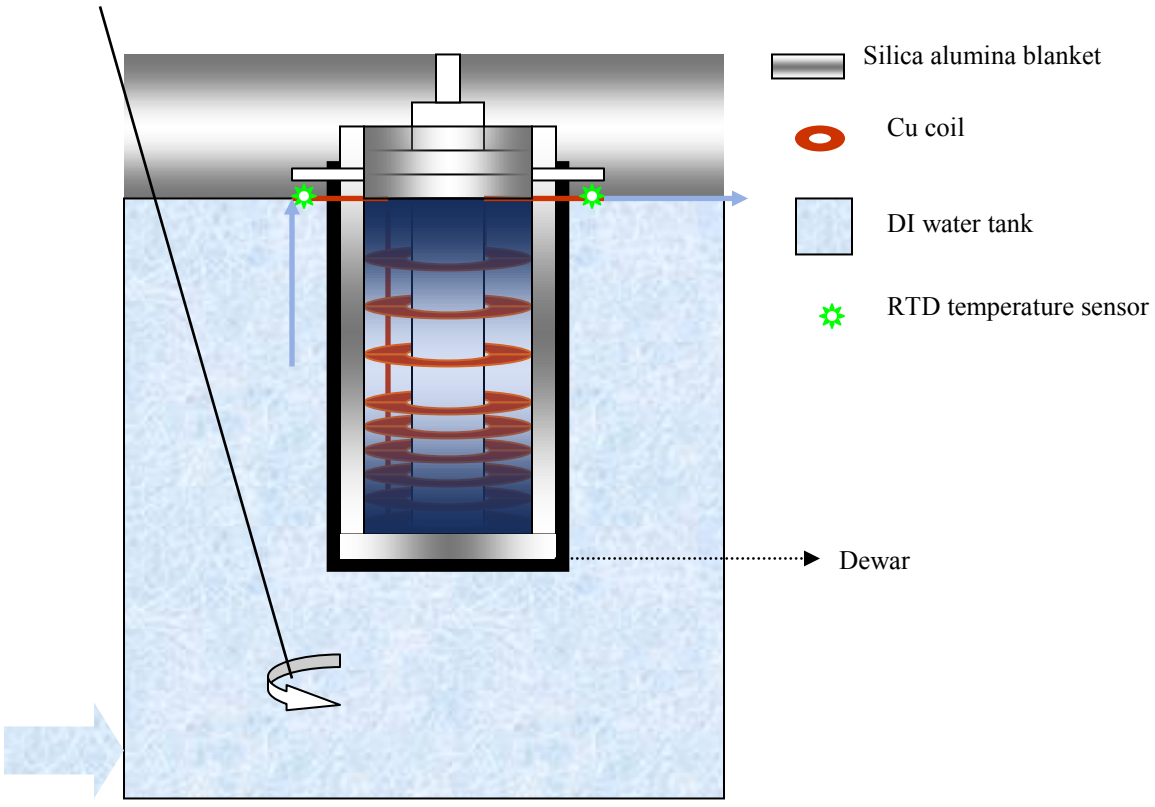

Figure 2. Flow calorimetry system and stirred constant-temperature bath.

A 0.25" o.d. copper coil wraps around the cylindrical stainless steel vessel, and the unit is held in a 1.5" i.d. ABS vessel containing ~ 30ml of water for heat transfer. The outside of the ABS vessel is insulated with a silica-alumina blanket, which forms a tight fit inside a 2-liter stainless steel Dewar flask. Finally, the calorimeter is immersed in a stirred 66 x 66 x 66-cm thermostatic water bath to a point below the edge of the Dewar flask. The parts of the calorimeter above the water level are also insulated with a silica-alumina blanket. An FMI 0SSY constant displacement pump draws the water through the copper coil from the bath to a reservoir on a computer-controlled 5–kg balance. When the reservoir is full, it automatically empties through an auto-siphon. The weight of the water in the reservoir and the time (with 1/60s resolution) is measured every minute.

The two RTD sensors measure the temperature at the inlet and outlet of the copper coil. The cell's electrolyte volume is ~ 20 cm^3.

CALIBRATION

After washing and rinsing, the cell was tested for leaks and filled with 20 cm^3 of 0.1 M LiOH solution in air at atmospheric pressure. Electrolysis current of 50, 100, and 175 mA was applied. The thermostatic bath was kept at 25°C, and the flow rate of the water was 0.28 ± 0.01 g/sec. Newtonian mass flow calorimetry calculations were performed on the results. The calorimeter shows an 83% heat recovery. This is to be expected since the calorimeter is not totally immersed in the bath because the cell's electrical connections are submersible. After applying this efficiency, the input and output powers are plotted in Figure 3.

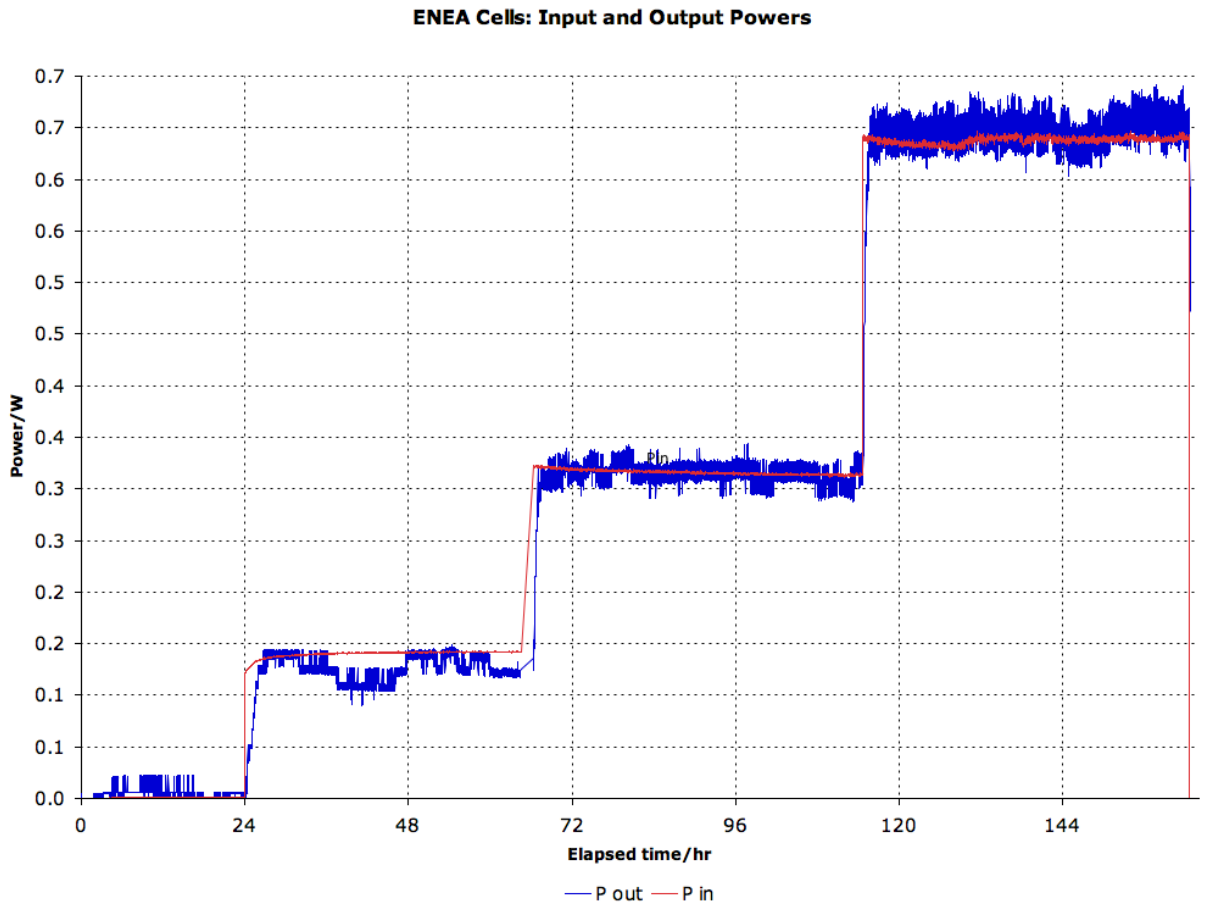

Figure 3. Input and output powers during the 4-step calibration.

ENEA MIXED ELECTROLYTE CELL

One of the cells from ENEA was set up and calibrated with H_2O electrolyte using direct current (DC) inside a mass flow calorimeter in a constant-temperature 200-liter bath. At the termination of that experiment, the cell was opened and 1 ml of D_2O added to the electrolyte. The cell was returned to the calorimeter and operated using a symmetric SuperWave™ designated "SW04". The cell was allowed to achieve thermal equilibrium for approximately 16 hours. The current was then raised to ~ 0.11A DC for approximately 12 hours. The current, flow rate, pressure, and R/R_0 are plotted versus elapsed time in days in Figure 4. At approximately 1.6 days, the Superwave™ was used to apply ~ 0.11A. At ~ 8.5 days 0.14A was applied using that same "SW04" wave. The cathode loading was not very high, although it is difficult to judge in the mixed H/D system. The pressure and slow rate were well behaved.

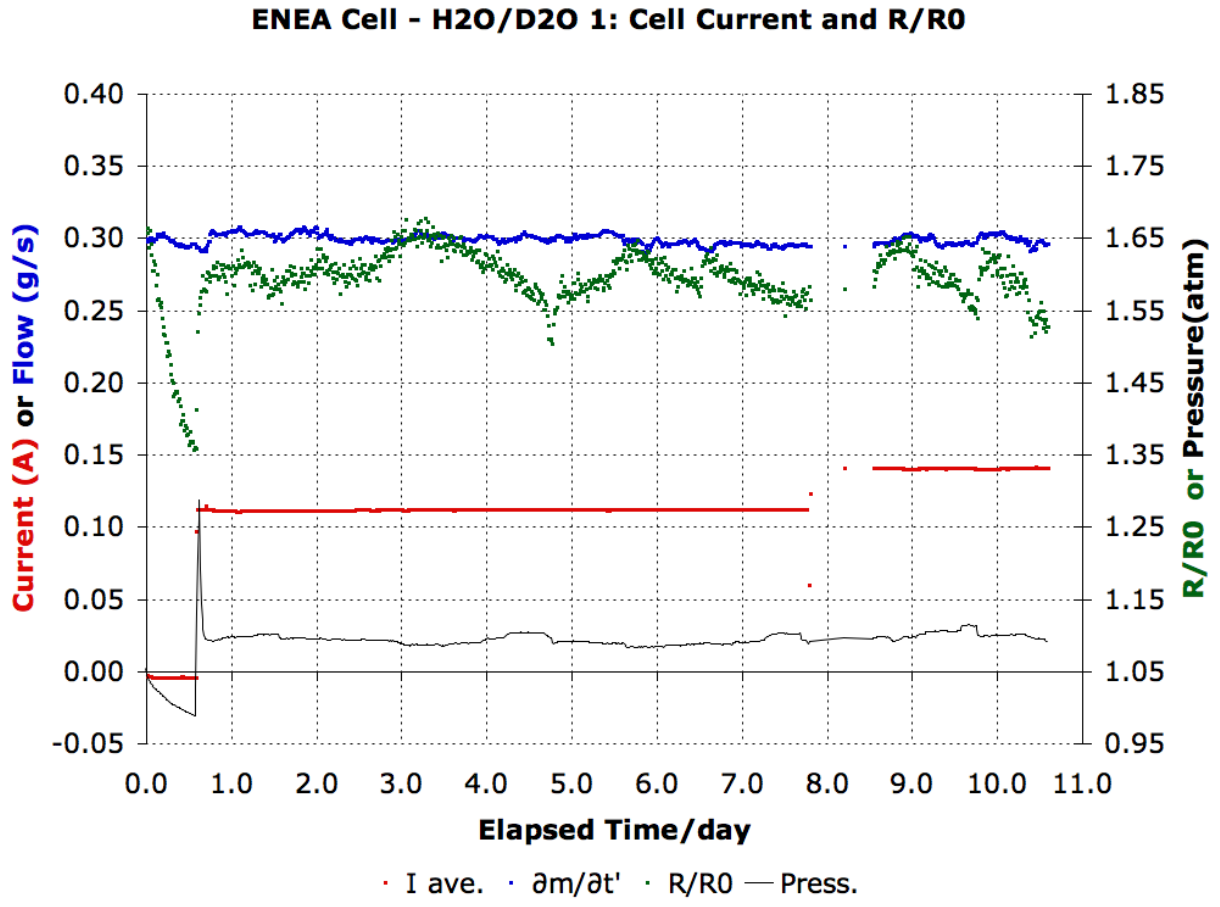

Figure 4. ENEA H_2O/D_2O cell current, pressure, flow rate and R/R_0.

The input power and output power, calculated using the calibration described earlier, are shown in Figure 5. It is possible that some excess power is seen starting approximately one day after the wave was applied. The scatter in this measurement prevents us from definitively declaring excess power.

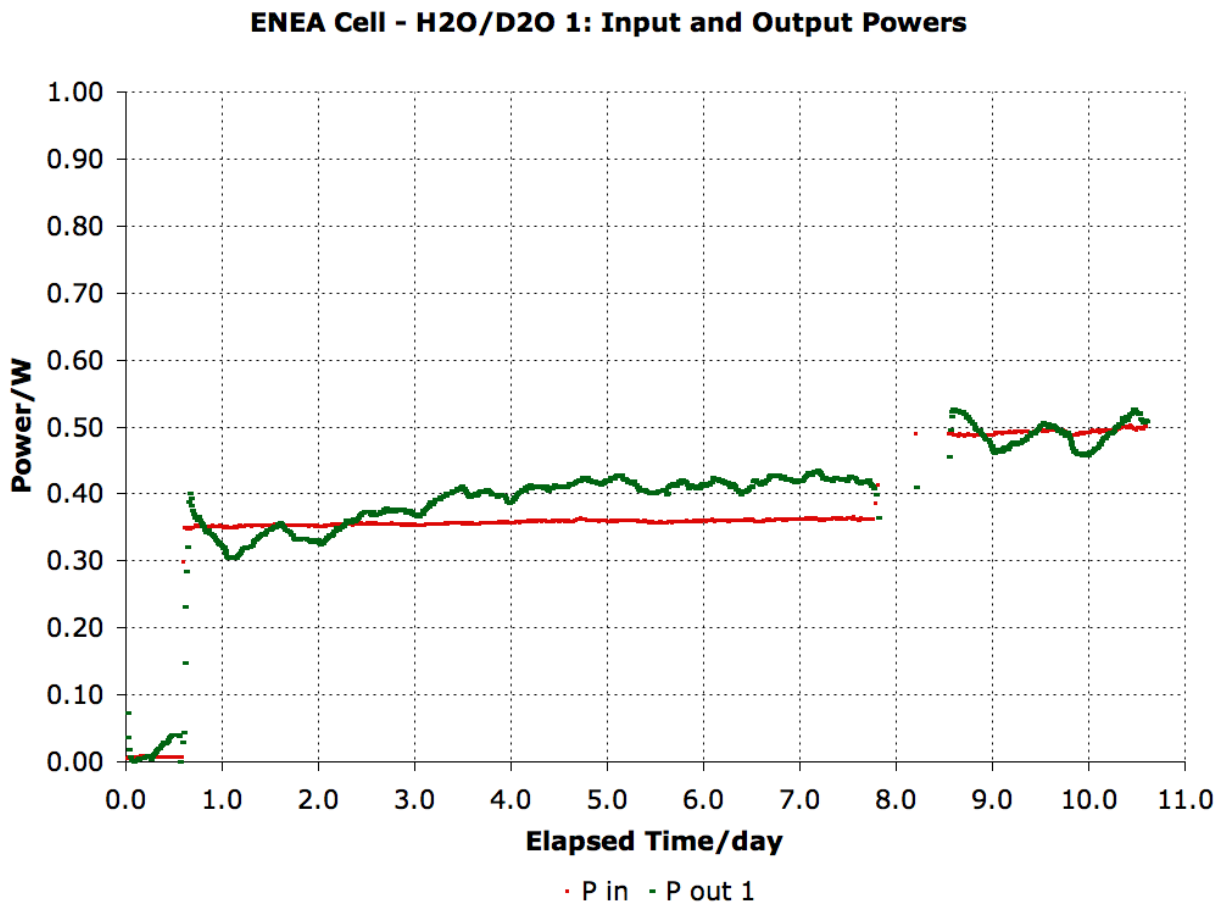

Figure 5. ENEA H_2O/D_2O cell input and output powers.

Using the cell that was calibrated with H_2O electrolyte inside a mass flow calorimeter in a constant-temperature 200-liter bath, we performed experiment "ENEA D_2O 1" using the L38 cathode provided by ENEA. This experiment was stimulated and loaded using the symmetric Superwave™ designated "SW04" shown in Figure 6 with steps up to ~ 2A (~ 220 ma/cm^2). The cell was allowed to achieve thermal equilibrium for approximately 48 hours. The current was then raised in steps of ~ 0.025A every 12 to 24 hours using SW04. The current, flow rate, pressure, and R/R_0 are plotted versus elapsed time in days in Figure 7. At the highest current, the voltage was unstable, which manifested itself as unstable power shown in Figure 8. The cathode loading was quite high, although the R/R_0 measurement became unstable at higher currents. The pressure and flow rate were well behaved.

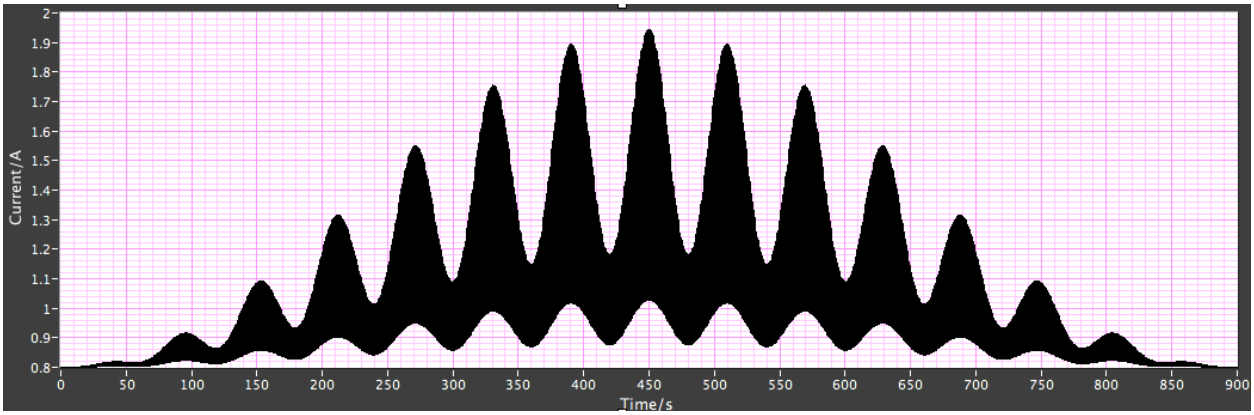

Figure 6. Superwave "SW04" used in the experiment described above.

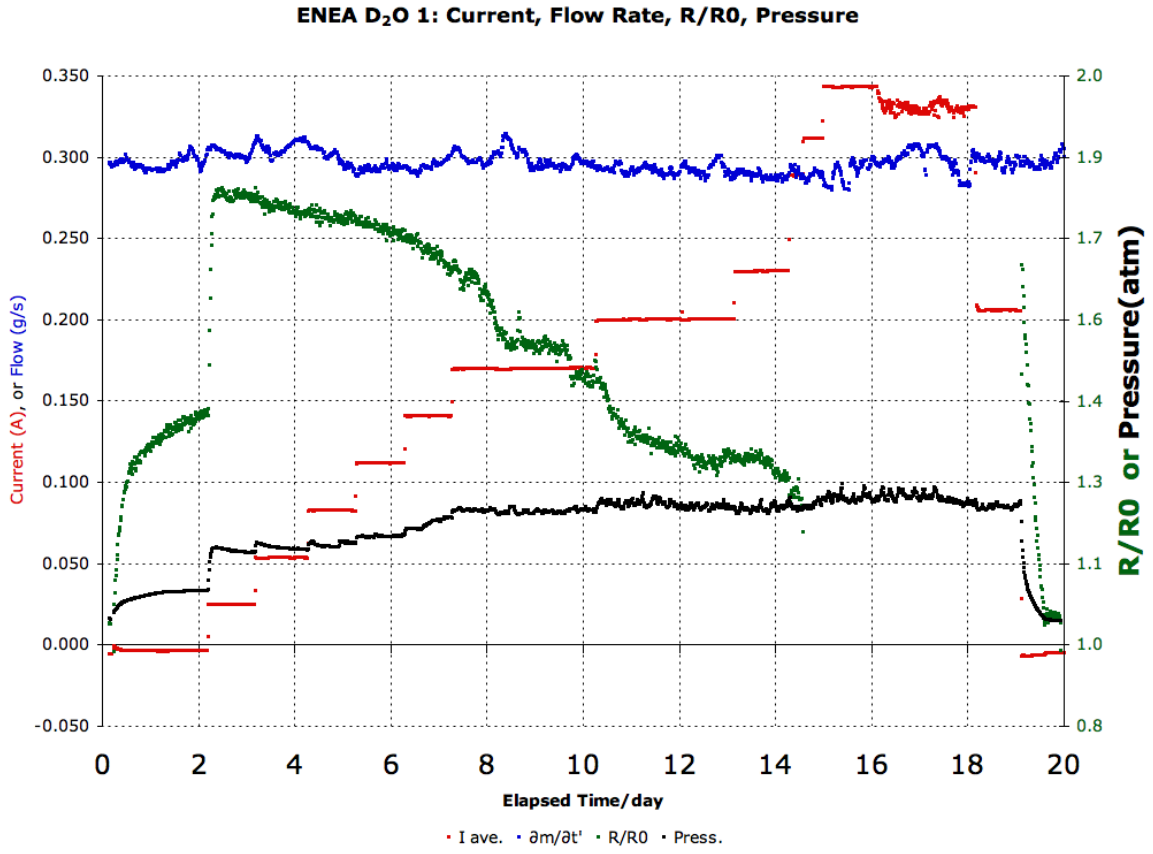

Figure 7. Current, R/R0, pressure, and flow rate from experiment "ENEA D2O 1".

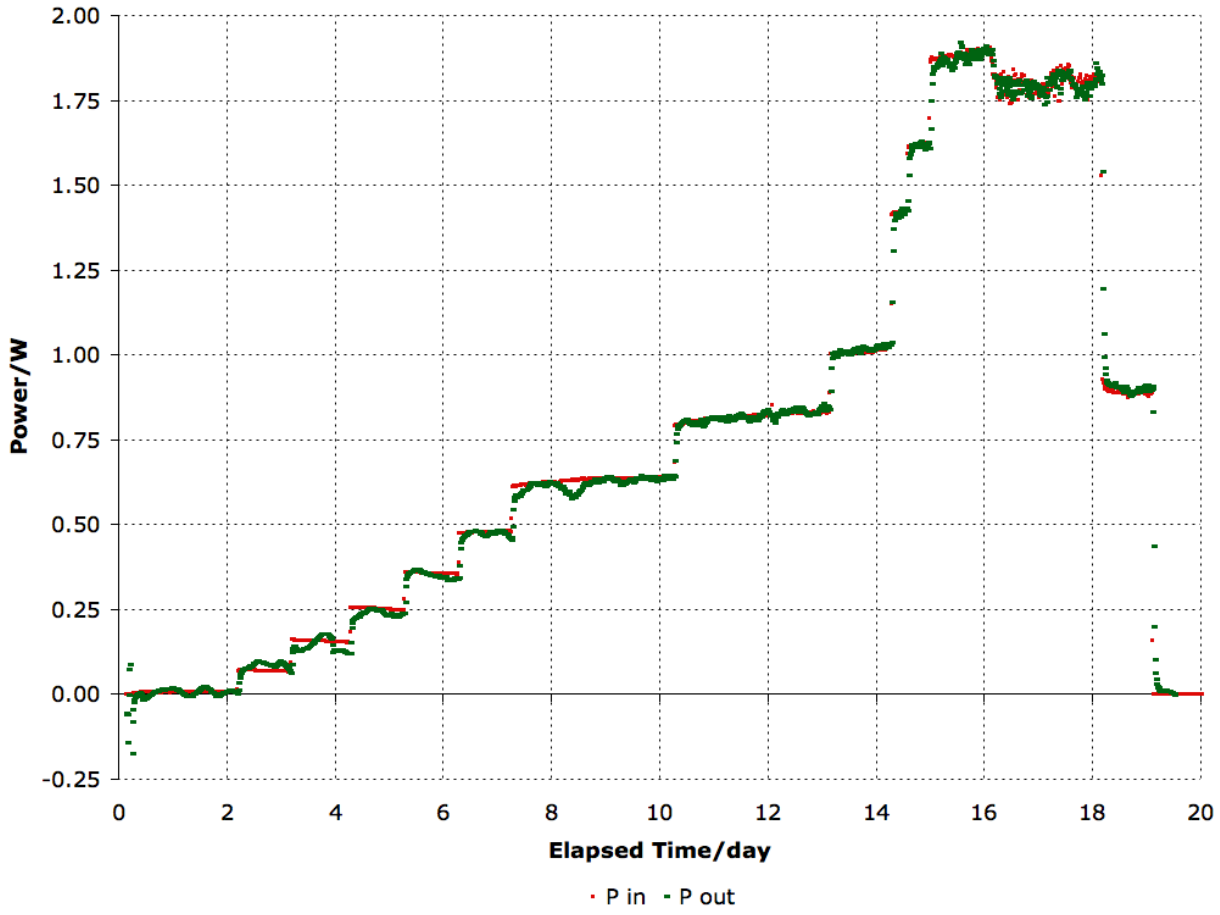

Figure 8. Input and output power from experiment "ENEA D2O 1".

CONCLUSIONS

Using SuperWave™ stimulation, very high loadings were obtained in both the D_2O and mixed H_2O/D_2O cells. Signs of excess power production were seen, but these signals were not very significant.

GAS-PHASE EXPERIMENTS WITH VARIOUS CATALYSTS

In early September 2009, Drs. Michael McKubre and Francis Tanzella visited Dr. Graham Hubler and his team at NRL. We met all day to discuss the design and future of the effort at NRL, as well as that at SRI. It was decided that due to preparations for the international conference in Rome in early October, effort on this task, as well as similar tasks at NRL, would be delayed until after the conference. Dr. Hubler suggested that SRI perform a literature study to ascertain what, if any, the field of ultra-sonic attenuation could contribute to this ultrasonic effort. These studies have been discussed with experts in the ultrasonic field.

SETUP AND OPERATION

As per discussions with Dr. Hubler, we initiated a reproduction of the recent work of Prof. Arata. We synthesized Pd on SiO_2 catalysts of four different Pd loadings. Table 1 shows the Pd loadings in these catalysts. Temperature profiles in these cells have been modeled by Dr. Violante in order to estimate the power output from each cell. The input power was held constant using a Hewlett Packard Model 66000 DC power supply, allowing up to 400 watts of power input.

We synthesized Pd on SiO_2 catalysts of four different Pd loadings as an analog of the Arata-style catalysts, which are on a ZrO_2 substrate. Table 1 shows the Pd loadings in these catalysts in which Pd nanoparticles are created on silica substrates by a sol-gel process. The wafers used in cell 4 with 2.5% Pd are shown in Figure 9. The calorimeters in their heating block and with gas/vacuum manifold attached are shown in Figure 10. Figure 11 shows a photograph of the pure silica wafers in the bottom of an open Matrix cell/calorimeter #1. The hole in the center of the wafer stack is for the thermowell.

Table 1. Palladium loading in analogs of Arata-style catalysts.

Cell #	1	2	3	4
Wt% Pd/SiO_2	0	0.7	1.5	2.5

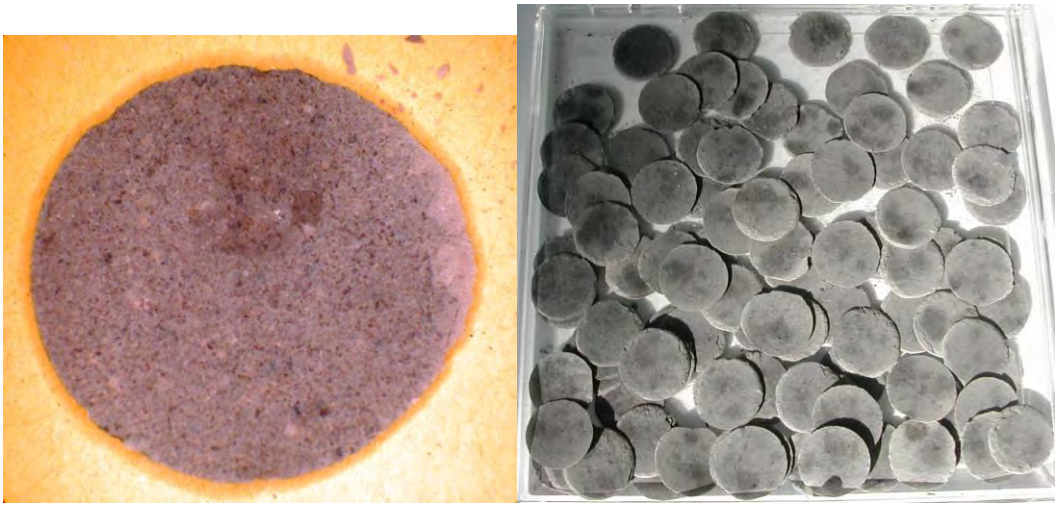

Figure 9. 2.5% Pd on silica wafers before loading into cell 4.

These catalysts were heated up to 300°C in several steps using SRI's "Matrix" calorimeters. Temperatures were measured in the catalyst bed and ~ 4 cm above the bed in a steel thermowell.

Figure 10. Matrix calorimeters in their heating block with the gas/vacuum manifold attached.

Figure 11. Silica wafers in open cell/calorimeter.

Figure 12 is a plot of the bed temperatures at the bottom of the four cells' thermowells and that of room temperature versus time. The temperature steps were usually separated by up to 48 hours to allow for equilibration of absolute temperatures. The temperature difference between that at the bottom of the thermowell and 4 cm above that point for all four cells is shown in Figure 13. This difference equilibrates much faster than the absolute temperatures. Plots of pressure versus time for the 4 cells are shown in Figure 14. Equivalent wafers of Pd on yttria-stabilized zirconia have been prepared for the subsequent set of experiments.

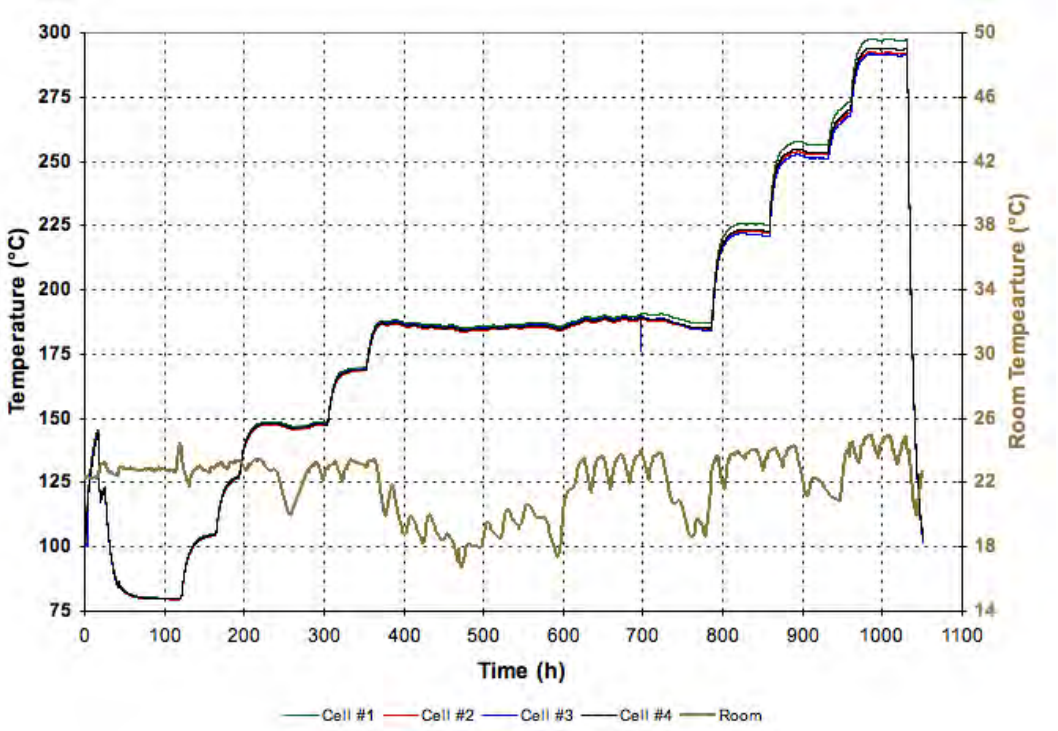

Figure 12. Bed and room temperature for the 4 matrix cell/calorimeters.

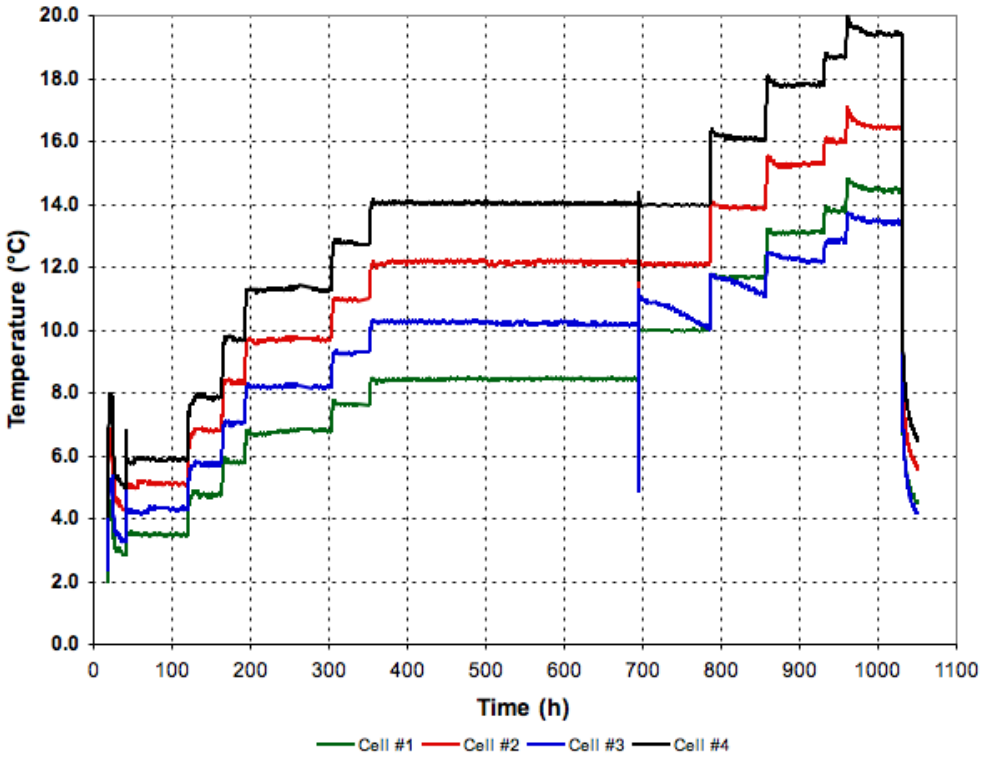

Figure 13. Temperature difference plot for the 4 matrix cell/calorimeters.

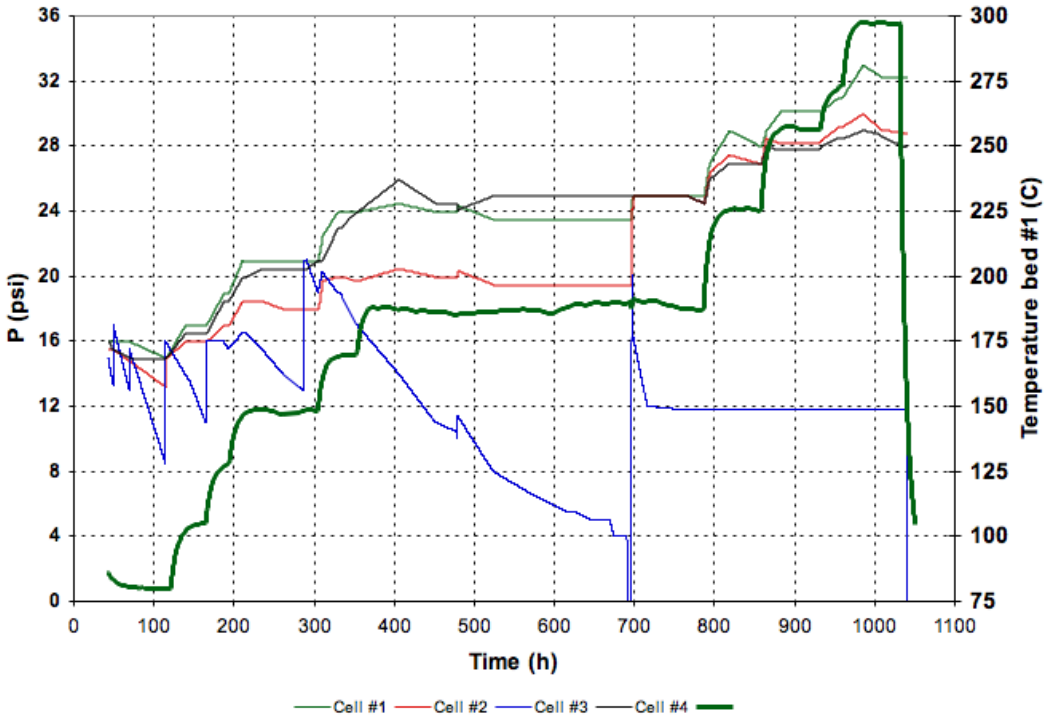

Figure 14. D2 Pressure plot for the 4 matrix cell/calorimeters.

MASS SPECTROSCOPY OF THE D_2 HEADSPACE GAS FROM THE PD ON SIO_2 CATALYSTS:

From the headspace gas samples taken from each cell, we have conducted the mass spectrometer (MS) analysis of He^3 and He^4. Table 2 shows the Pd loadings in SiO_2 along with the concentration of He^4 and He^3.

Table 2. Catalyst composition and He concentrations.

	Composition	He^4, ppm	He^3, ppt
Cylinder	D_2	0.26	37.5
Cell #1	0 wt% Pd/SiO_2	2.81	12.5
Cell #2	0.7 wt% Pd/SiO_2	1.40	35.1
Cell #3	1.5 wt% Pd/SiO_2	4.87	5.6
Cell #4	2.5 wt% Pd/SiO_2	0.78	30.4

In the analysis of the data from MS, several cautions must be taken:

1) After 700 h of running the D_2 exposure test, the D_2 cylinder was changed. Before adding the new D_2, the D_2 already in the vessels containing the SiO_2 and Pd/SiO_2 catalysts was evacuated for 5 minutes at the temperature of 190°C.

2) The analysis of He^3 gave a broad range of ppt values. In the case of the D_2 cylinder, the range varied from 7 to 60 ppt. The suspected presence of tritium would explain this behavior since the getter installed in the preparation sample of the MS would remove it. The final concentration would depend on the time allowed to the sample to be in contact with this getter before entering the MS.

3) The cell #3 leaked during the experiment, and the MS analysis shows values of He^3 and He^4 close to those in air.

H_2 EXPOSURE EXPERIMENTS ON THE PD ON SIO_2 CATALYSTS:

Immediately after the D_2 exposure experiment, the samples were exposed to H_2 starting at room temperature following similar procedure to that used in the D_2 exposure.

Figure 15 shows a plot of the bed temperatures at the bottom of the four cells' thermowells and that of room temperature versus time. The temperature steps were usually separated by up to 48 hours to allow for equilibration of absolute temperatures. The temperature difference between that at the bottom of the thermowell and 4 cm above that point for all four cells is shown in Figure 16. This difference equilibrates much faster than does the absolute temperatures. Figure 17 shows the H_2 pressure for the four cells versus time. The pressure gauge for cell #3 was not operating properly such that those results are not reliable. Also, the pressure in cell #3 exceeded the 30 psi maximum value of the gauge.

During the cooling process at the end of the D_2 exposure experiment, the welded thermocouple broke, and the new one was supposedly installed at the same 4-cm gap apart. The greater delta-T for the cell#1 was due to the misplacement of that thermocouple. We conducted an experiment with D_2 at two temperatures, and it does confirm the misplacement of the thermocouple in the shaft vessel of cell#2.

The cells follow the same delta-T pattern as in the D_2 experiments: Cell #4 with the highest concentration of Pd has the highest delta-T.

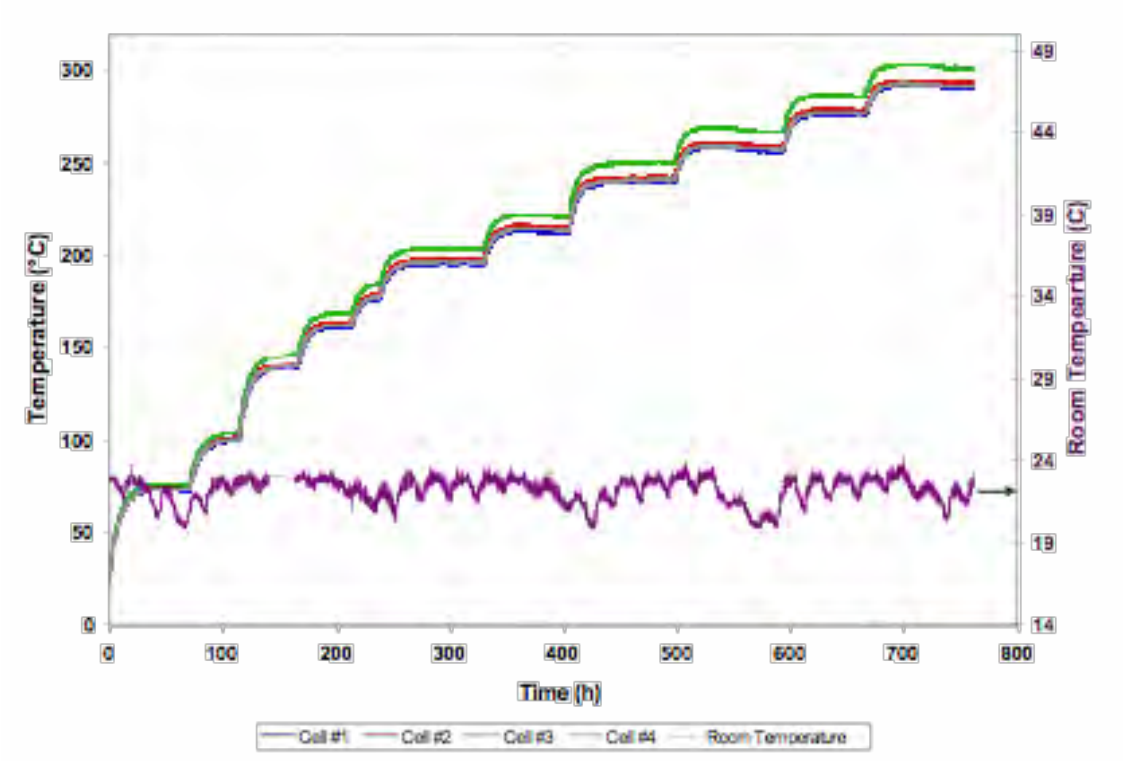

Figure 15. Bed and room temperature for the 4-matrix cell/calorimeter.

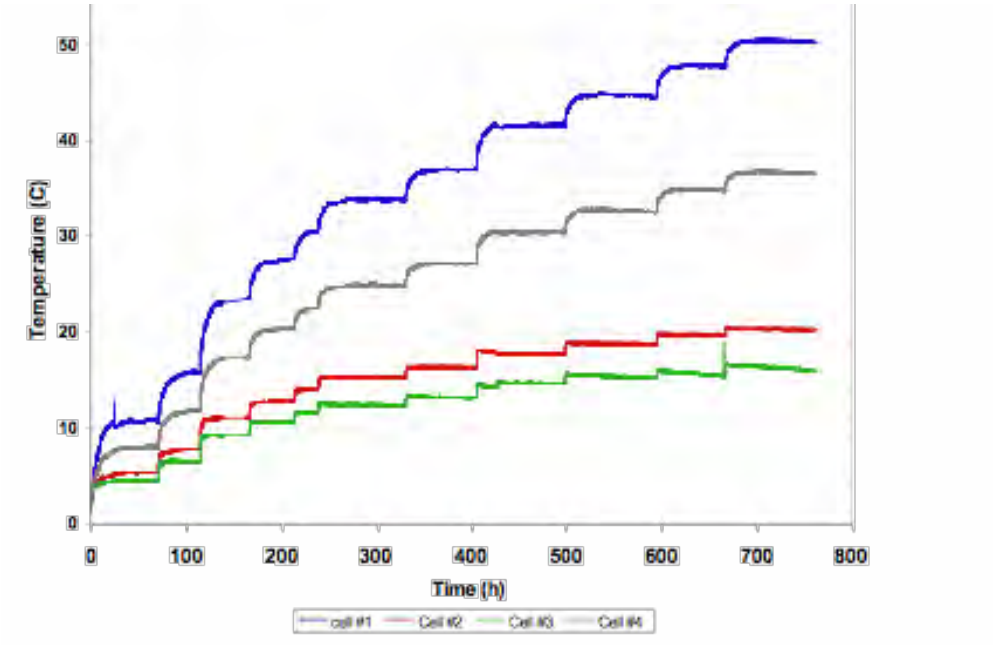

Figure 16. Temperature difference plot for the 4 matrix cell/calorimeter.

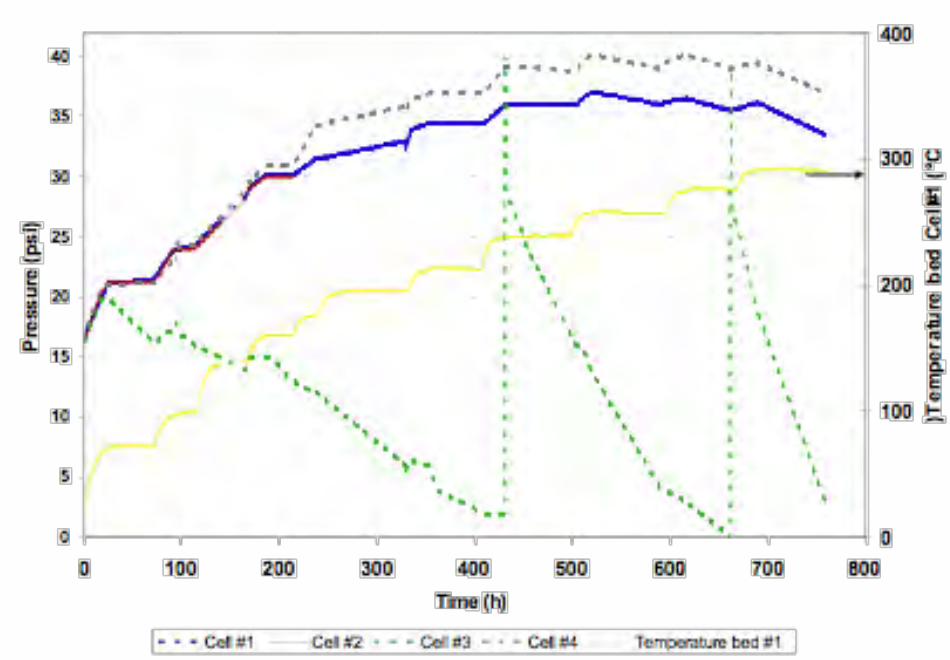

Figure 17. H_2 Pressure plot for the 4 matrix cell/calorimeter.

After having completed the SiO2 analog of the Arata-style catalysts experiments, we prepared zirconia based catalysts using yttria stabilized zirconia (YSZ). Pd-exchanged zeolite samples were prepared by the conventional cation exchange procedure using two methods: (1) fast reduction (change of pH and increase of temperature) of ionic Pd on the zeolites, and (2) slow reduction (no pH change and room temperature) of ionic Pd on the zeolites

The specifications of the zeolites are shown in Table 3. The percentage of Pd deposited on the zeolites following Methods 1 and 2 is shown in Table 4.

Table 3: Zeolite Specifications.

Zeolite	SiO_2/Al_2O_3 molar ratio	W% Na_2O	Surface area $m^2.g^{-1}$
Y type 1	5.21	2.8	730
Y type 2	5.2	0.2	660
Y type 3	80	0.03	780
Beta type	360	0.05	620
Mordenite	90	0.05	500

Table 4: Pd Concentration Deposited on Different Zeolites.

Zeolite	Pd w% Method 1	Pd w% Method 2
Y type 1	0.4	-
Y type 2	6.6	5.5
Y type 3	5.9	2.1
Beta type	2.3	4.7
Mordenite	2.5	3.5

The Pd exchange rate was close to 100% for the type-2 zeolite sample although the rate of exchange can be improved by increasing the time for the cation exchange process. Figures 18 – 20 show the original zeolites and the two types of Pd-exchanged zeolites.

Figure 18. Original zeolites.

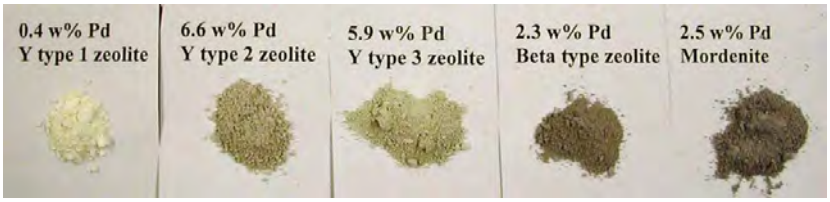

Figure 19. Pd on zeolites following Method 1.

Figure 20. Pd on zeolites following Method 2.

XRD ANALYSIS

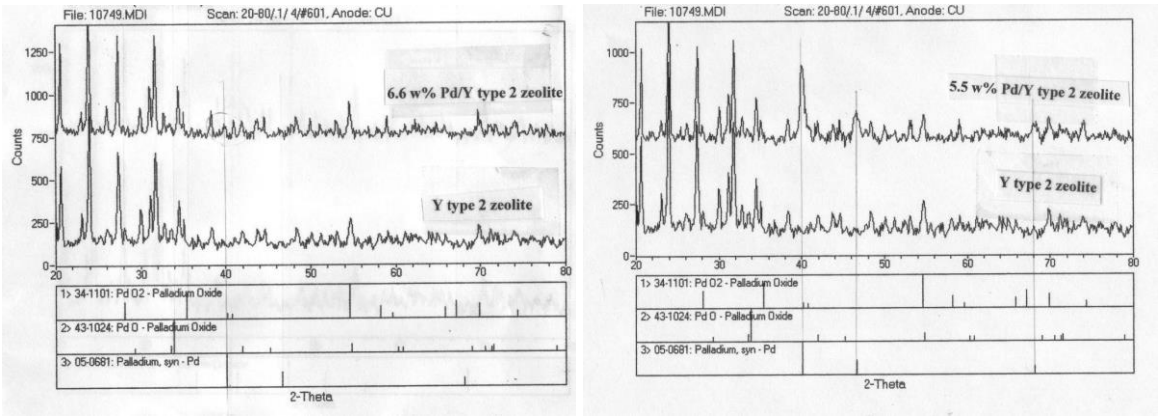

Figure 21. XRD pattern of Pd-exchange Y-type 2 zeolite: (Right) Method 1: (Left) Method 2.

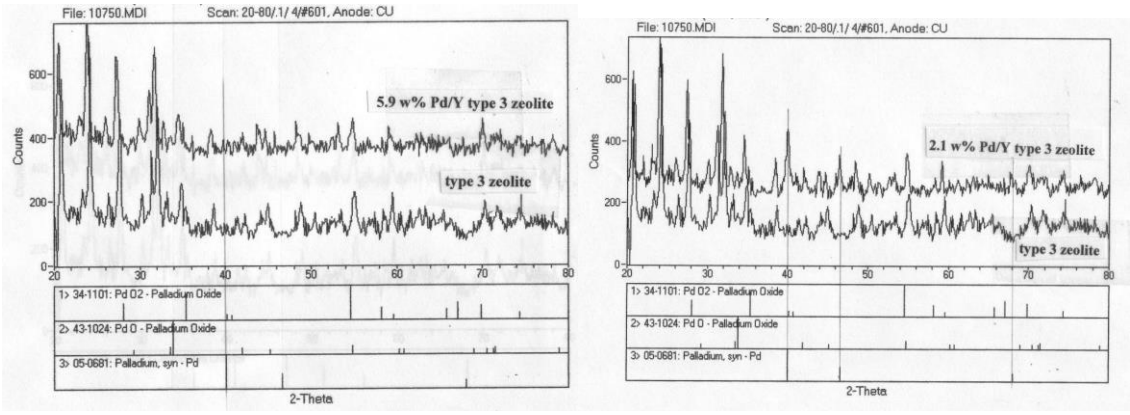

Figure 22 .XRD pattern of Pd-exchange Y-type 3 zeolite: (Right) Method 1: (Left) Method 2.

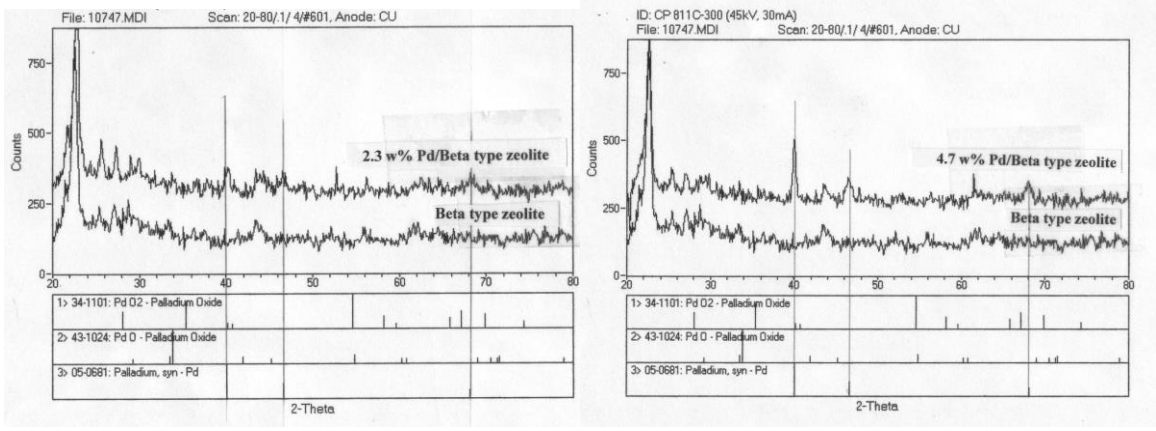

Figure 23. XRD pattern of Pd-exchange Beta-type zeolite: (Right) Method 1: (Left) Method 2.

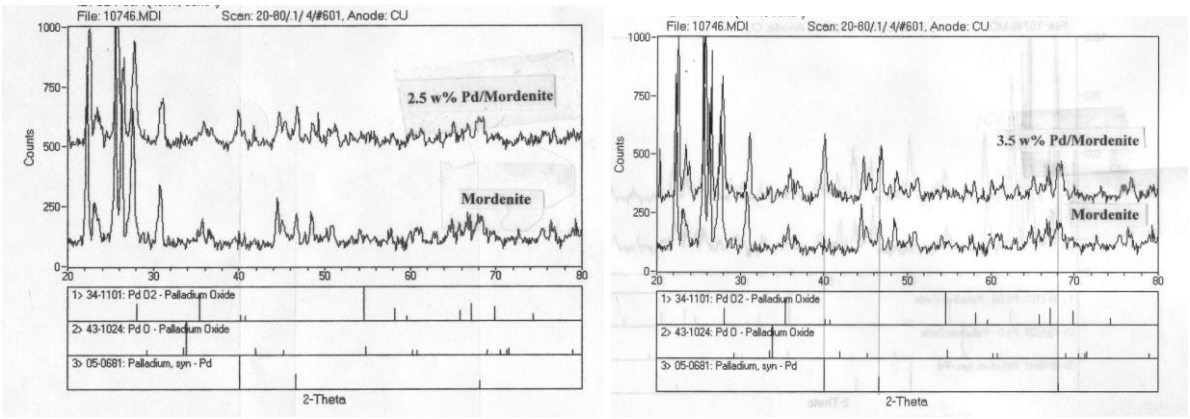

Figure 24. XRD pattern of Pd-exchange mordenite: (Right) Method 1: (Left) Method 2.

From this work, we draw the following conclusions:

1) The lower the Na_2O content in zeolite, the higher the amount of Pd exchanged. The Y-type 1 zeolite presented the lowest amount of Pd on zeolite (Tables 3 and 4). No further preparation of Pd-exchanged Y-type 1 zeolite was performed.

2) The difference between Methods 1 and 2 for Pd-exchanged type 2 zeolite: The percentage of Pd in the zeolite is similar, 6.6 and 5.5 wt% from Methods 1 and 2 respectively (Table 4) but the peak of Pd metal from Method 1 is smaller than that from Method 2 (Figure 21). The exchange rate is high in both cases, but the reduction rate of Pd^{2+} is lower in Method 1.

3) The difference between Methods 1 and 2 for Pd-exchanged type 3 zeolite: The percentage of Pd in the zeolite varies from 5.9 wt% from Method 1 to 2.1 wt% from Method 2 (4 2). The exchange rate of Pd is higher in Method 1 but the XRD pattern shows no Pd metal just PdO. On the other hand, the Pd exchanged zeolite from Method 2 resulted in Pd metal (Figure 22).

4) The difference between Methods 1 and 2 for Pd-exchanged beta-type zeolite: In this sample, the percentage of Pd is higher from Method 2: 4.7 wt% compared to 2.3 wt% from Method 1 (Table 4). Contrary to the Y-type zeolites, the rate of Pd exchange is higher now from Method 2. In both Methods, the Pd is present as Pd metal (Figure 23).

5) The difference between Methods 1 and 2 for Pd-exchanged mordenite: In this sample, again the percentage of Pd is higher from Method 2: 3.5 wt% compared to 2.5 wt% from Method 1 (Table 4). Contrary to Y-type zeolites and similar to the beta-type, the rate of Pd exchange is higher now in Method 2. In both Methods, the Pd is present as Pd metal (Figure 24).

D_2 ABSORPTION EXPERIMENTS WITH PD/ZEOLITE 13X AND ZEOLITE 13X FROM NRL LAB

We have performed two consecutive adsorption/desorption experiments using 1 wt% Pd/zeolite 13x (NRL #H120-24h-AD 1%Pd-X13-00011910B) and one adsorption/desorption experiment using zeolite 13x (NRL #X13 Blank).

The procedure consisted first of removing most of the water by heating at 110°C, then introducing D_2 at about 83 psig, and holding it for 10 minutes before expanding the gas from the sample vessel into a known volume (~ 150% of the vessel volume) and the vessel sealed. The sample vessel is held at a constant 40°C. After the He content of this expanded gas was analyzed by the MS, the gas was pumped away and the expansion volume evacuated to ~ 10^{-5} torr. After

each analysis, the remaining gas from the vessel was expanded into the expansion volume and vessel was again sealed. This procedure included a MS determination of the concentration of He-4 and He-3 after each expansion. This procedure not only allowed us to determine the concentration of He isotopes for each new pressure, but to estimate the total amount of He removed from the vessel and thus determine an approximate mass balance.

For the first experiment, we used 6.5 g of received material (containing approximately 15 wt% water). The XRD of the Zeolite 13x and the Pd/Zeolite 13x are similar, and no Pd peak was detected in the latter material as shown in Figure 25.

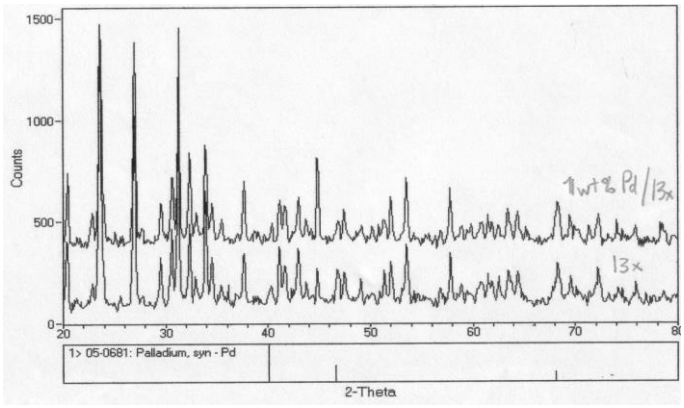

Figure 25. XRD pattern of 1 wt% Pd/zeolite 13 and zeolite 13x.

D_2 adsorption/desorption on 1 wt% Pd/zeolite 13x #1a

The D_2 pressure of the vessel containing the material varied from 6.8 to 3.10^{-3} atm over 13 expansions. Figure 26 shows the evolution of moles of He-4 and its concentration in the vessel with the consecutives gas expansion/dilution. Analyses of the D_2 cylinder found 0.15 ppm of He-4.

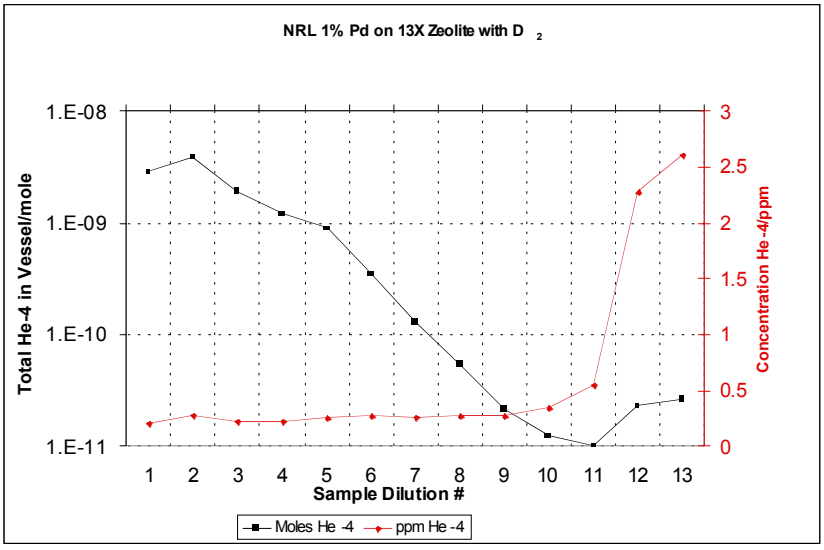

Figure 26. Evolution of He4 moles in the vessel and He4 concentration with the dilutions for the 1st D2 adsorption/desorption experiment on 1 wt% Pd/zeolite 13x.

D_2 adsorption/desorption on 1 wt% Pd/Zeolite 13x #1b

In this D_2 adsorption/desorption experiment, the 1wt% Pd/Zeolite 13x sample used in the experiment described above was pumped to 10^{-7} torr overnight and exposed to a similar expansion protocol. The vessel was first filled with D_2 gas to 6.6 atm and held for 10-15 minutes. The pressure was reduced to 1 x 10^{-3} atm over 12 expansions. The He-3 and He-4 concentration was determined by MS analysis at every dilution. Figure 27 shows the number of moles of He^4 and its concentration in the vessel with each consecutive gas expansion/dilution.

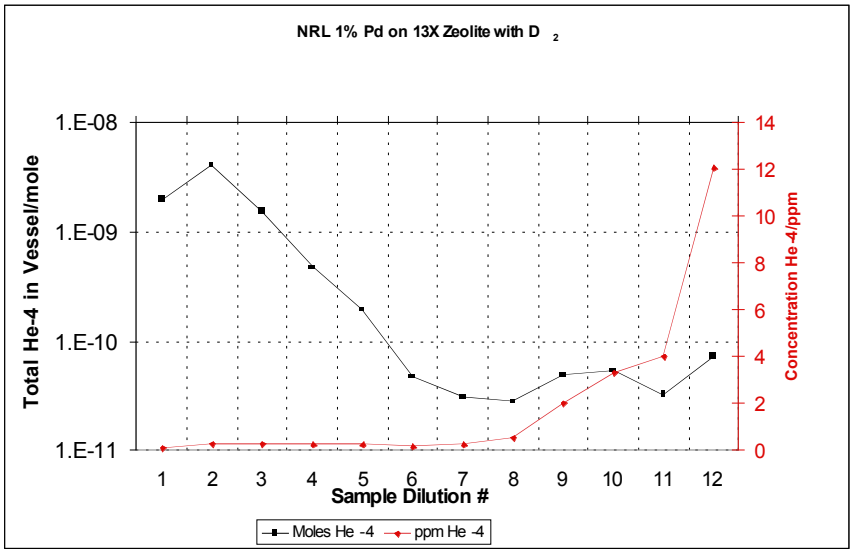

Figure 27. Evolution of He4 moles in the vessel and He4 concentration with the dilutions for the 2nd D2 adsorption/desorption experiment on 1 wt% Pd/zeolite 13x.

D_2 adsorption/desorption on Zeolite 13x (Blank test)

We followed the same procedure using Zeolite 13x as supplied by Dr. Kidwell at NRL. The D_2 pressure of the vessel containing the material varied from 6.7 to 3.10^{-3} atm over 9 expansions. Figure 28 shows the number of moles of He^4 and its concentration in the vessel with each consecutive expansion/dilution.

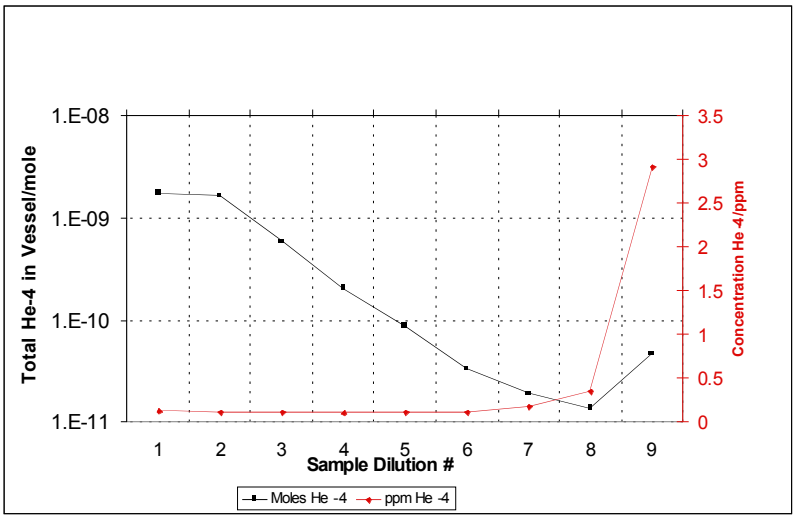

Figure 28. Evolution of He^4 moles in the vessel and He^4 concentration with the dilutions for the D_2 adsorption/desorption experiment on zeolite 13x.

D_2 absorption experiments with Pd/zeolite 13x and zeolite 13x from NRL

We have continued our analysis of He-4 and He-3 in the headspace above D_2 over Pd on zeolites as prepared by D. Kidwell. Dr. Kidwell spent approximately one week at SRI working with us to perform these tasks. Table 5 summarizes the mass balance from these results. The experiments designated NRL1 – NRL4 were performed using different manifold volumes that the other experiments these earlier experiments used a flow-through carbon cryo-trap as opposed to the cold finger type cryo-trap used in the latter experiments. These results have been sent to Dr. Kidwell for analysis.

Table 5. Helium measurement results from $D_2(H_2)$/Pd/zeolite experiments.

Sample	Designation	Gas	He^4 moles IN	He^4 moles OUT
H120-24h AD 1%Pd-x13-00011910B	NRL1 (5/27)	D_2	2.59×10^{-9}	3.04×10^{-9}
	NRL2 (6/1)	D_2	1.74×10^{-9}	1.92×10^{-9}
X13-zeolite	NRL3 (6/8)	D_2	1.51×10^{-9}	1.24×10^{-9}
H120-24h AD 1%Pd-x13-00011910B	NRL4 (6/15)	D_2	3.28×10^{-10}	2.69×10^{-10}
H120-24h AD 1%Pd-x13-0060310B	NRL5a (8/21)	D_2	4.87×10^{-9}	3.93×10^{-9}
	NRL5b (8/23)	D_2	4.29×10^{-9}	1.08×10^{-8}
	NRL5c (8/24)	D_2	3.37×10^{-11}	2.45×10^{-10}
	NRL6 (8/31)	H_2	2.20×10^{-10}	1.79×10^{-10}
	NRL7 (9/10)	D_2	8.18×10^{-11}	6.23×10^{-11}

CONCLUSIONS

After operating tens of experiments, we have found that D_2 exposure to Pd-filled zeolites and $PdNiZrO_x$ catalysts leads to higher temperatures than does H_2 exposure. However, we have not ruled out that this may be due to heat capacity and thermal conductivity differences between the two gases.